



THE UNIVERSITY *of* EDINBURGH

Edinburgh Research Explorer

## Evaluating the performance of honeycomb briquettes produced from semi-coke and corn stover char

### Citation for published version:

Cong, H, Zhao, L, Mašek, O, Yao, Z, Meng, H, Huo, L, Yuan, Y, Jia, J & Wu, Y 2021, 'Evaluating the performance of honeycomb briquettes produced from semi-coke and corn stover char: Co-combustion, emission characteristics, and a value-chain model for rural China', *Journal of Cleaner Production*, vol. 244, 118770. <https://doi.org/10.1016/j.jclepro.2019.118770>

### Digital Object Identifier (DOI):

[10.1016/j.jclepro.2019.118770](https://doi.org/10.1016/j.jclepro.2019.118770)

### Link:

[Link to publication record in Edinburgh Research Explorer](#)

### Document Version:

Peer reviewed version

### Published In:

Journal of Cleaner Production

### General rights

Copyright for the publications made accessible via the Edinburgh Research Explorer is retained by the author(s) and / or other copyright owners and it is a condition of accessing these publications that users recognise and abide by the legal requirements associated with these rights.

### Take down policy

The University of Edinburgh has made every reasonable effort to ensure that Edinburgh Research Explorer content complies with UK legislation. If you believe that the public display of this file breaches copyright please contact [openaccess@ed.ac.uk](mailto:openaccess@ed.ac.uk) providing details, and we will remove access to the work immediately and investigate your claim.



1 **Evaluating the performance of honeycomb briquettes produced from**  
2 **semi-coke and corn stover char: Co-combustion, emission**  
3 **characteristics, and a value-chain model for rural China**

4  
5 Hongbin Cong<sup>a</sup>, Lixin Zhao<sup>a,\*</sup>, Ondřej Mašek<sup>b</sup>, Zonglu Yao<sup>a</sup>, Haibo Meng<sup>a</sup>, Lili Huo<sup>a</sup>,  
6 Yanwen Yuan<sup>a</sup>, Jixiu Jia<sup>a</sup>, Yunong Wu<sup>a</sup>

7 <sup>a</sup>Center of Energy and Environmental Protection, Chinese Academy of Agricultural  
8 Engineering Planning & Design, Beijing 100125, China

9 <sup>b</sup>University of Edinburgh, School of Geosciences, UK Biochar Research Centre,  
10 King's Buildings, Edinburgh EH93FF, UK

11

12 **\*Corresponding author:** Tel./fax: +86 010 59196810.

13 E-mail address: zhaolixin5092@163.com

14

15

16

17

18

19

20

21

22           **ABSTRACT:** A honeycomb briquette made from semi-coke and corn stover  
23 char was developed as a possible heating fuel in rural China. In this study, the co-  
24 combustion characteristics of semi-coke and corn stover char combined in different  
25 proportions were tested and analyzed. It was determined that adding 20 % corn stover  
26 char (BS28) effectively improved the combustion performance of semi-coke, and this  
27 proportion was regarded as the ideal mixing ratio. Thus, the integrated combustion  
28 characteristics of the blend improved to  $15.08 \times 10^{-12} \text{ K}^{-3} \cdot \text{min}^{-2}$  compared to  $5.44 \times 10^{-12}$   
29  $\text{K}^{-3} \cdot \text{min}^{-2}$  for semi-coke alone. The emission test results revealed that  $\text{SO}_2$  and  $\text{PM}_{2.5}$   
30 emissions decreased with corn stover char addition; however,  $\text{NO}_x$  emissions  
31 increased and the combustion efficiency decreased slightly with corn stover char  
32 addition. The  $\text{SO}_2$  concentrations resulting from the combustion of BriqCK, Briq28,  
33 and Briq46 (honeycomb briquettes with ratios of char to semi-coke of 0:10, 2:8, and  
34 4:6, respectively) under different experimental conditions were 24.9–26.3, 9.5–16.7,  
35 and 5.2–15.4  $\text{mg}/\text{Nm}^3$ , respectively, and the  $\text{NO}_x$  concentrations were 63.1–149.7,  
36 54.3–175.4, and 57.7–168.4  $\text{mg}/\text{Nm}^3$ , respectively. A value-chain model for the new  
37 heating fuel was developed and possible benefits were analyzed. If either the new  
38 investment cost or raw material input costs (\$25 USD/t of straw char) were subsidized  
39 by national public finance, then the project would be profitable and run sustainably.  
40 This study provided an important technical basis for the development and application  
41 of new heating fuels in China.

42

43 **Keywords:** co-combustion; air pollution emission; corn stover char; semi-coke;  
44 honeycomb briquette<sup>1</sup>

## 45 **1. Introduction**

46 The amount of collectible crop straw (e.g., from corn, wheat, rice, and cotton) in  
47 China was approximately 900 million tons during recent five years (MOA, 2016). A  
48 large amount of crop straw has been burned directly in open fields. This open field  
49 burning has serious implications for air pollution, traffic accidents, and overall fire  
50 risk. Instead of open field burning, if these crop residues were properly utilized as  
51 fuel, then China's reliance on coal as a primary energy source would be expected to  
52 decrease (Chen, 2016; Sun, 2016). Straw char produced by slow pyrolysis consists  
53 mainly of carbon, minerals, and metals (EBC, 2018; Klinghoffer et al., 2011). There  
54 are numerous beneficial possibilities for its use, including waste management, climate  
55 change mitigation, and clean energy production (Gómez et al., 2016; Kua et al., 2019;  
56 Li et al., 2019). Owing to properties that make it a clean and renewable fuel, it is  
57 feasible to explore efficient methods, such as densification, to upgrade straw char into  
58 high value-added bioenergy (Hu et al., 2015). The widespread use of straw char  
59 requires the development of adequate utilization strategies to achieve economic and  
60 environmental sustainability of bioenergy chains (Barbanera et al., 2018).

61 The Chinese government's 13th Five-Year Plan for Energy Development  
62 proposes to replace conventional coal with clean energy sources, including natural

---

<sup>1</sup>Originally a honeycomb-shaped block molded using only coal, which is the main household fuel for many residents in East Asia.

63 gas, electric power, clean coal, and renewable energy, for heating in northern China  
64 (NEA, 2017). Semi-coke is an industrial product of bituminous raw coal produced by  
65 low-temperature carbonization (Jie et al., 2018). It is considered a potential  
66 replacement for raw coal (MEP, 2016) because it has a high fixed carbon content,  
67 high calorific value, and low ash, sulfur, and phosphorus contents. Replacing  
68 traditional raw coal with semi-coke briquettes could effectively improve  
69 environmental outcomes (Li et al., 2016; Li et al., 2016a), as the use of semi-coke  
70 briquettes has the potential to reduce emissions compared with those from current  
71 coal consumption in China (Jie et al., 2018).

72 Straw char's high alkali and alkaline earth metals (AAEMs) content may cause  
73 several operating problems in the combustion system (Hernández et al., 2016);  
74 however, they can weaken the polymer chain and catalyze the combustion of semi-  
75 coke (Peng et al., 2015). Compared with semi-coke, straw char has higher  
76 hydrophobicity but lower densification performance (Hu, 2015). Despite the large  
77 number of studies on the co-combustion characteristics of biomass with char, sludge,  
78 and oil shale (Liu et al., 2015; Niu et al., 2017; Sarkar et al., 2014), there remains a  
79 considerable knowledge gap in the development of a new fuel blended from straw  
80 char and semi-coke, which are produced by similar processes using different raw  
81 feedstocks. Information pertaining to the emissions from the combustion of  
82 honeycomb briquettes produced from a combination of semi-coke and straw char is  
83 also very limited (Li et al., 2016a; Yank, 2016), which affects the development and

84 promotion of new heating fuels.

85 The primary objective of this study was to investigate the influence of variations  
86 in corn stover char blending proportions on the combustion characteristics of semi-  
87 coke, and to determine the emission characteristics of a new honeycomb briquette  
88 molded from a combination of corn stover char and semi-coke. In addition, a value-  
89 chain model for honeycomb briquette production and utilization was designed, and  
90 the expected benefits based on the model were analyzed. This provided essential data  
91 for the development and application of a new heating briquette produced from a  
92 combination of straw char and semi-coke.

## 93 **2. Materials and methods**

### 94 ***2.1 Characterization of materials***

95 The test materials primarily included corn stover char, semi-coke, and  
96 honeycomb briquettes molded from different blends of these two fuels. Corn stover  
97 char was produced using a pilot-scale rotary kiln at a pyrolysis temperature of 600 °C  
98 and a residence time of 30 min (Cong et al., 2017). Semi-coke was obtained directly  
99 from the market; it was produced by low-temperature carbonization of highly volatile  
100 bituminous coal from Shenmu County, Shaanxi Province, which is the largest semi-  
101 coke production base in China. Blends of corn stover char and semi-coke for the  
102 combustion characteristics test were marked with BC $\times\times$  (Table 1). Based on the  
103 results of the co-combustion characteristics analysis, the ratios of corn stover char to  
104 semi-coke of 2:8 and 4:6 (BS28 and BS46) were selected for analysis in the pollution

105 emission study, and the blends were molded into honeycomb briquettes with a  
 106 pressure of 21kN; meanwhile, honeycomb briquettes molded from semi-coke alone  
 107 were also used for comparative analysis. The honeycomb briquettes were marked with  
 108 Briq×× (Table 1). Finally, 6 % kaolin and 1.5 % glutinous rice flour (by mass) were  
 109 added to the main ingredients to improve the densification performance when the  
 110 honeycomb briquettes were molded.

111 **Table 1.** Summary of abbreviations used for the various mixtures and honeycomb  
 112 briquettes

Abbreviations	BS28	BS46	BS64	BS82	BriqCK	Briq28	Briq46
Corn straw char: semi-coke (by mass)	2:8	4:6	6:4	8:2	0:10	2:8	4:6

113

114 Before compression molding, the raw materials were milled through a 4 mm  
 115 mesh. Table 2 presents the characteristics of the raw materials. Heating values were  
 116 measured using a bomb calorimeter (LECO AC-300) following the adiabatic method  
 117 according to the China national standard (GB T 213-2008). The ultimate analysis  
 118 (carbon, hydrogen, nitrogen, and sulfur) was determined using a Vario ELIII  
 119 Elemental Analyzer according to ASTM 5373 and ASTM 4239. The metal element  
 120 contents were determined by inductively coupled plasma mass spectrometry (Thermo  
 121 Fisher Scientific) according to AOAC Official Method 975. 03.

122

123 **Table 2.** Characteristics of the raw materials

Material		Corn stover char	Semi-coke
Particle size [mm]		≤4	≤4
Bulk density <sup>a</sup> [kg/m <sup>3</sup> ]		264.79	750.28
LHV <sup>b</sup> [MJ/kg]		22.53	23.32
Proximate analysis [wt % ad]	Moisture	2.78	10.28
	Volatile	10.08	13.97
	Ash	31.81	19.89
	Fixed carbon	55.33	55.86
Ultimate analysis [wt % daf]	C	65.86	70.04
	H	2.19	0.46
	O <sup>c</sup>	30.45	28.60
	N	1.46	0.62
	S	0.04	0.28
Metal elements [mg/g]	Na	1.35	0.23
	K	35.23	0.12
	Ca	23.02	0.48
	Mg	11.46	0.02
	Al	2.32	0.02
	Si	0.11	0.01

124 ad: air-dry basis; daf: dry and ash-free basis

125 <sup>a</sup>Tested according to the methods of the dust character test (the China national



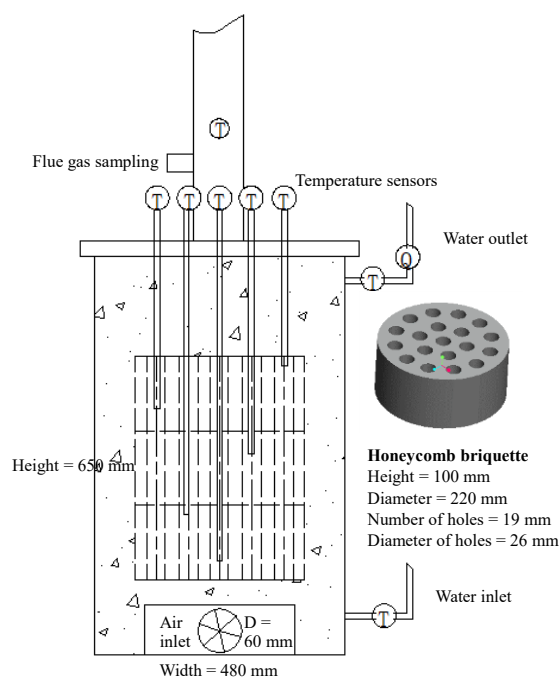
126 standard GB/T16913-2008)

127 <sup>b</sup>LHV: lower heating value

128 <sup>c</sup>Calculated by the difference

## 129 ***2.2 Experimental facility***

130 An NF9C household heating stove (Laowan Biomass Technology Co., Ltd.,  
131 China) was used in this study; raw coal briquettes are frequently used to power this  
132 type of stove in rural areas of northern China. The stove had a hearth height of 650  
133 mm, an outer length × width of 480×480 mm, and an inner diameter of 230 mm (Fig.  
134 1). It had an enclosed combustion chamber, circulating water system, and an air inlet  
135 with a diameter of 60 mm near the stove bottom. The air inlet was set up with open  
136 ratios of 0 %, 40 %, 70 %, and 100 % during various experiments to examine  
137 emissions. Special honeycomb briquettes with a height of 100 mm, an outer diameter  
138 of 220 mm, and 19 holes with a diameter of 26 mm were used in this study.



139

140 **Fig. 1.** Testing system based on a household heating stove from rural China using the  
 141 special honeycomb briquettes.

142

### 143 **2.3 Analytical methods**

144 In this study, a thermogravimetric analyzer (STA409PC) manufactured by  
 145 NETZSCH was used to analyze the combustion characteristics, and the test results  
 146 were smoothed using Proteus 5.3 software. The reactor had a diameter of 60 mm, and  
 147 the reaction atmosphere was canned air. The surface of the crucible (6 mm inner  
 148 diameter) was uniformly coated with 5–10 mg samples and then covered with a  
 149 platinum cap provided by NETZSCH. The initial temperature of the test was set at  
 150 30 °C; it was raised to 930 °C at a heating rate of 10 °C/min. The air flow rate was  
 151 100 mL/min. These settings were similar to those used in previous related studies

152 (Niu et al., 2017; Sarkar et al., 2014).

153 Total suspended particles (TSP) were collected using an electrical low-pressure  
154 impactor (Dekati ELPI+) manufactured by DEKATI Ltd., which can collect particles  
155 from 6 nm to about 10  $\mu\text{m}$  in 14 size fractions. The mass size distributions and the  
156 number size distributions of the TSP were estimated using ELPI software V12.0. To  
157 ensure that the collected particulate matter was kept below saturation, the flue gas was  
158 diluted 64 times using two Dekati diluters.

159 A flue gas analyzer (ECOM-J2KN) manufactured by RBR was used to test the  
160  $\text{NO}_x$ ,  $\text{SO}_2$ , CO, and  $\text{CO}_2$  emissions, and the flue gas was sampled three times, once  
161 every 4 minutes. The results were converted from ppm to  $\text{mg}/\text{Nm}^3$ .

162 Combustion characteristics were evaluated using several combustion parameters  
163 (e.g., ignition temperature, burnout temperature, burnout characteristics, and  
164 integrated combustion characteristics), as previously described (Moon et al., 2013).  
165 The burnout index ( $C_b$ ) ( $10^{-4}/\text{min}$ ) was used to characterize the burnout characteristics  
166 of the sample; large values indicated a greater burnout performance.

167 
$$C_b = \frac{f_1 \cdot f_2}{t_0}, \quad (1)$$

168 where  $f_1$  (%) is the initial burnout rate, which characterizes the loss rate of fuel weight  
169 on the ignition point of the thermogravimetry (TG) curve (a large value represents  
170 greater flammability of the fuel);  $f_2$  (%) is the late burnout rate; and  $t_0$  (min) is the  
171 burnout time, which represents the time from the initiation of combustion mass loss to  
172 burnout (with a mass loss rate of 98 %).

173 The integrated combustion characteristics of the sample were described by the  
174 combustion index ( $S_N$ ) ( $10^{-12} \text{ K}^{-3} \cdot \text{min}^{-2}$ ); larger values indicated a greater burning  
175 performance of the sample.

$$176 \quad S_N = \frac{(dw/dt)_{max} \cdot (dw/dt)_{mean}}{t_i^2 t_f}, \quad (2)$$

177 where  $(dw/dt)_{max}$  (%/min) is the maximum burn rate,  $(dw/dt)_{mean}$  (%/min) is the  
178 average burn rate,  $t_i$  (K) is the ignition temperature, and  $t_b$  (K) is the burnout  
179 temperature.

180 The China national standard GB 18484-2001 was used to calculate the CE  
181 (combustion efficiency; %) based on the concentrations of CO and CO<sub>2</sub>.

$$182 \quad CE = \frac{C_{CO_2}}{C_{CO_2} + C_{CO}} \times 100 \%, \quad (3)$$

183 where  $C_{CO_2}$  and  $C_{CO}$  are the test concentrations of CO<sub>2</sub> and CO in the flue gas (%),  
184 respectively.

### 185 **3. Results and discussion**

#### 186 **3.1 Co-combustion characteristics**

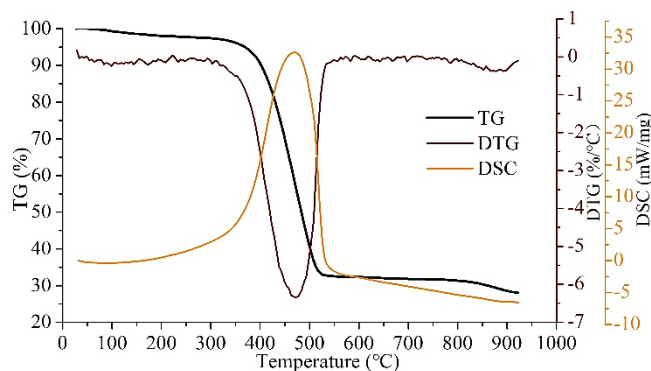
##### 187 3.1.1 Combustion characteristic curves of corn stover char and semi-coke

188 The thermogravimetry (TG), differential thermogravimetry (DTG), and  
189 differential scanning calorimetry (DSC) curves of the semi-coke and corn stover char  
190 were tested. As shown in Fig. 2, the weight loss and exothermic processes of the two  
191 fuels were clearly different. When the samples were heated, water evaporated, which  
192 was accompanied by devolatilization, volatile flaming, and fixed carbon firing (Zhao  
193 et al., 2014). Before the heating temperature reached 100 °C, the semi-coke

194 experienced a high reduction in weight owing to the loss of its relatively high  
195 moisture content (Table 1). Corn stover char exhibited a more intense rate of weight  
196 loss during the second stage; this occurred at a relatively lower temperature than that  
197 for semi-coke.

198 The char exhibited a faster rate of weight loss and a narrower exothermic  
199 duration. The combustion performance of corn stover char was better than that of  
200 semi-coke. The burnout characteristic index and the integrated combustion index of  
201 the char were  $100.17 \times 10^{-4}/\text{min}$  and  $35.73 \times 10^{-12} \text{ K}^{-3} \cdot \text{min}^{-2}$ , respectively, while the two  
202 indexes of the semi-coke were  $48.28 \times 10^{-4}/\text{min}$  and  $5.44 \times 10^{-12} \text{ K}^{-3} \cdot \text{min}^{-2}$ , respectively.

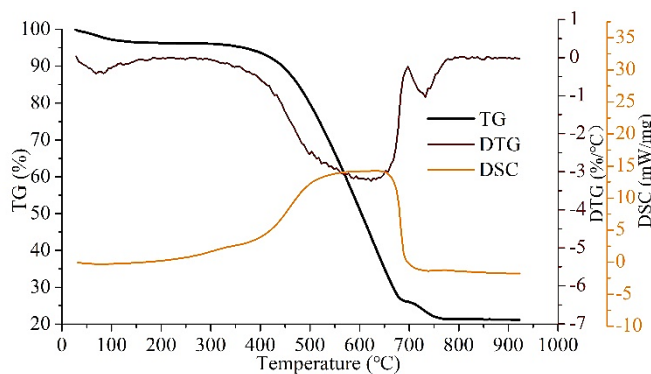
203



204

205

(a)



206

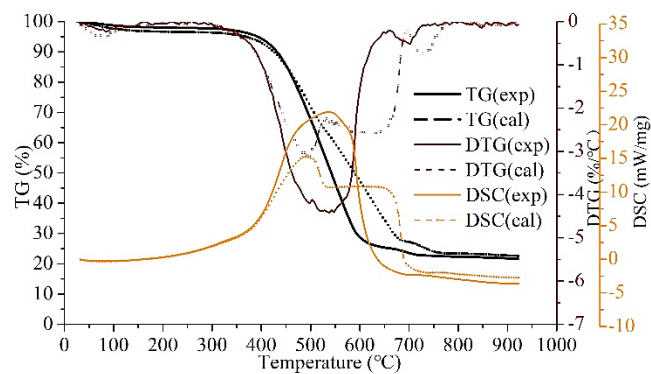
207

(b)

208 **Fig. 2.** Combustion characteristic curves (The thermogravimetry (TG), differential  
209 thermogravimetry (DTG), and differential scanning calorimetry (DSC) curves ) of  
210 corn stover char (a) and semi-coke (b).

### 211 3.1.2 Co-combustion curves and their interaction

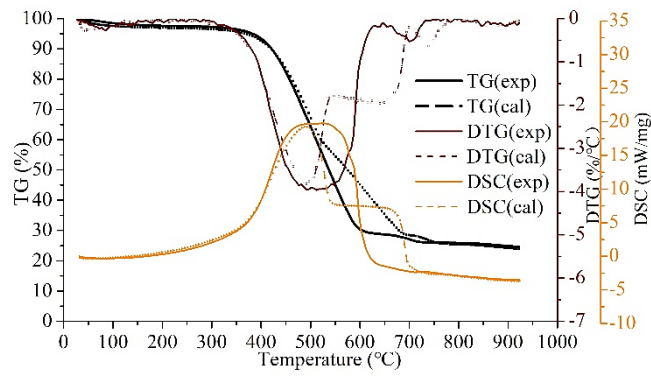
212 The theoretical thermogravimetry ( $TG_{cal}$ ) curves, theoretical differential  
213 thermogravimetry ( $DTG_{cal}$ ) curves, and theoretical differential scanning calorimetry  
214 ( $DSC_{cal}$ ) curves were calculated using the proportional superposition method based on  
215 the ratio of corn stover char to semi-coke and test results presented in Fig. 2 (Xing et  
216 al., 2019), and were compared with the test-derived curves ( $TG_{exp}$ ,  $DTG_{exp}$ , and  
217  $DSC_{exp}$ ). These are all shown in Fig. 3.



218

219

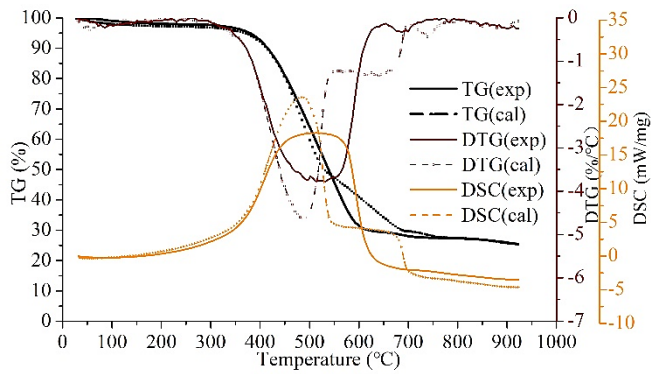
(a)



220

221

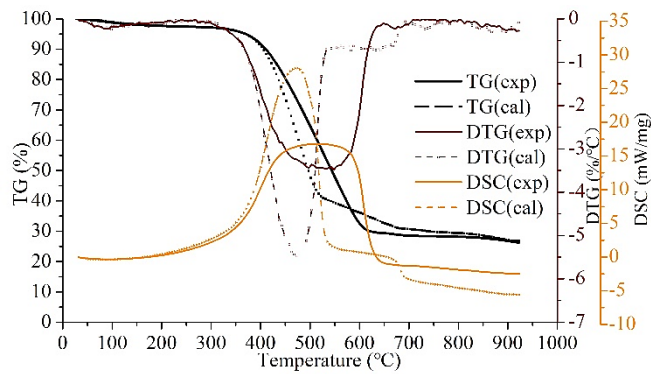
(b)



222

223

(c)



224

225

(d)

226 **Fig. 3.** Theoretical (subscripted with cal) and test-derived (subscripted with exp) co-

227 combustion characteristic curves (thermogravimetry (TG), differential

228 thermogravimetry (DTG), and differential scanning calorimetry (DSC) curves) of

229 blends BS28 (a), BS46 (b), BS64 (c), and BS82 (d).

230 All test-derived TG curves were smoother than the theoretical TG curves, thereby  
231 indicating that there was an interaction between the two fuels during their co-firing.  
232 Furthermore, the test-derived  $TG_{exp}$  curve of BS28 shifted distinctly to the left of the  
233  $TG_{cal}$  curve, and this phenomenon was also reflected in the DSC and DTG curves.  
234 The peaks of the  $DSC_{exp}$  and  $DTG_{exp}$  curves were distinctly larger than those of the  
235  $DSC_{cal}$  and  $DTG_{cal}$  curves for BS28. As the proportion of corn stover char increased,  
236 the extent of the left shift of the curve decreased. Consequently, the  $TG_{exp}$  curves of  
237 BS46 and BS64 were similar to the  $TG_{cal}$  curves. By contrast, the  $TG_{exp}$  curve of  
238 BS82 showed a distinct shift to the right, and this phenomenon was also reflected in  
239 the DSC and DTG curves. The peaks of the  $DSC_{exp}$  and  $DTG_{exp}$  curves were smaller  
240 than those of the  $DSC_{cal}$  and  $DTG_{cal}$  curves for BS82, respectively.

241 According to the above analysis, it was apparent that when the proportion of char  
242 was less than 40 % of the total, the combustion performance of the semi-coke  
243 improved. However, a small amount of semi-coke added to char (20 % in the test)  
244 resulted in a strong inhibition of char combustion. This might have been due to the  
245 fact that some AAEMs (e.g., potassium, sodium, calcium, and magnesium) in the  
246 straw char weakened the polymer chain and catalyzed the combustion of semi-coke  
247 (Mourant et al., 2011; Peng et al., 2015), while a small amount of semi-coke hindered  
248 the diffusion of the flame during char combustion, thereby exhibiting a distinct flame  
249 retardant effect (Sarkar et al., 2014).



250 3.1.3 Co-combustion characteristic indexes

251 Table 3 shows the combustion characteristic indexes of different samples. The  
 252 ignition temperature decreased from 429.1 °C (BS28) to 404.9 °C (BS82) as the  
 253 proportion of char increased, which was consistent with the theoretical trend.  
 254 However, the burnout characteristic indexes decreased as the proportion of char  
 255 increased, and ranged from  $54.78 \times 10^{-4}/\text{min}$  for BS28 to  $48.49 \times 10^{-4}/\text{min}$  for BS82.  
 256 The maximum and average reaction rates also showed similar trends. In addition, the  
 257 integrated combustion indexes of BS28, BS46, BS64, and BS82 were 15.08, 13.53,  
 258 12.27, and  $10.31 \times 10^{-12} \text{ K}^{-3} \cdot \text{min}^{-2}$ , respectively, which indicated a contradictory  
 259 tendency when compared with the theoretical values. The quantitative study also  
 260 demonstrated that a small amount of char addition ( $\leq 40\%$ ) was more effective at  
 261 improving the combustion characteristics of semi-coke than the addition of a large  
 262 amount of char ( $\geq 60\%$ ), even though the combustion characteristics of corn stover  
 263 char were distinctly better than those of semi-coke.

264 **Table 3.** Combustion indexes of the samples

Sample	Ignition temperature (°C)	Burnout temperature (°C)	Burnout characteristics ( $C_b$ ) ( $10^{-4}/\text{min}$ )	Maximum reaction rate $(dw/dt)_{\text{max}}$ (%/min)	Average reaction rate $(dw/dt)_{\text{mean}}$ (%/min)	Integrated combustion characteristics ( $SM$ ) ( $10^{-12} \text{ K}^{-3} \cdot \text{min}^{-2}$ )
Semi-coke	459.1	693.1	48.28	-3.27	-2.43	5.44
BS28	429.1	601.4	54.78	-4.42	-3.78	15.08
BS46	414.0	593.8	50.00	-3.97	-3.47	13.53
BS64	410.8	595.5	52.76	-3.79	-3.25	12.27
BS82	404.9	603.1	48.49	-3.48	-2.93	10.31
Biochar	401.6	518.1	100.17	-6.35	-4.70	35.73

265

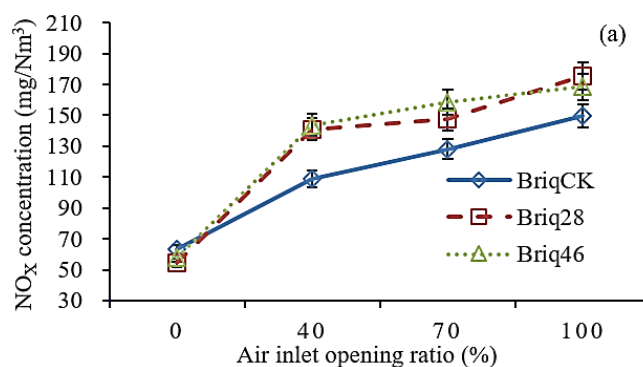
## 266 *3.2 Air pollution emissions of honeycomb briquettes*

### 267 3.2.1 Conventional gaseous pollutant emissions

268 NO<sub>X</sub> and SO<sub>2</sub> emissions are generally regarded as the main conventional gaseous  
269 pollutants. As the opening ratio of the air inlet increased, the NO<sub>X</sub> concentrations of  
270 all briquettes increased (Fig. 4a). The NO<sub>X</sub> concentrations of BriqCK, Briq28, and  
271 Briq46 were 63.1–149.7, 54.3–175.4, and 57.7–168.4 mg/Nm<sup>3</sup>, respectively, as the  
272 opening ratio increased from 0 % to 100 %. This trend could be explained as follows.  
273 First, at temperatures below 1300 °C, only fuel-NO<sub>X</sub> was expected (De Soete, 1990;  
274 Werther, 2000) and the correlation between fuel nitrogen and NO<sub>X</sub> emissions was  
275 significant (Roy, 2012). The nitrogen content in corn stover char was more than  
276 double that found in semi-coke. With the increasing proportion of corn stover char,  
277 the fuel nitrogen content of the honeycomb briquettes increased, thereby causing  
278 increased NO<sub>X</sub> concentrations (Jin et al., 2016). The NO<sub>X</sub> emissions from biomass  
279 may be lower or higher than those from coal owing to the fact that the nitrogen  
280 content of different biomasses varies widely (Ren et al., 2017). Second, the stove  
281 temperature increased with the increasing opening ratio of the air inlet, and the higher  
282 flame temperature resulted in more NO<sub>X</sub> being generated (Courtemanche and  
283 Levendis, 1998). However, the NO<sub>X</sub> concentrations for the new fuels were always  
284 lower than the limiting value of 200 mg/Nm<sup>3</sup> of the China national standard (GB  
285 2014-4365) under all experimental conditions.

286 The SO<sub>2</sub> concentrations of BriqCK, Briq28, and Briq46 under different

287 experimental conditions were 24.9–26.3, 9.5–16.7, and 5.2–15.4 mg/Nm<sup>3</sup>,  
 288 respectively (Fig. 4b). Overall, the SO<sub>2</sub> emissions were highest from BriqCK and  
 289 lowest from Briq46. With the increasing proportion of corn stover char, the SO<sub>2</sub>  
 290 concentration decreased. The sulfur content in the char was approximately 15 % of  
 291 that in the semi-coke. The SO<sub>2</sub> emissions varied as a function of fuel-bound sulfur,  
 292 and the AAEMs in corn stover char were potent absorbers of SO<sub>2</sub> (Tarelho et al.,  
 293 2005; Werther, 2000; Zhang et al., 2019). The SO<sub>2</sub> emissions of Briq28 and Briq46  
 294 exhibited a weak downward trend as the opening ratio of the air inlet increased; the  
 295 higher flame temperature enhanced the SO<sub>2</sub> capture ability of the AAEMs (Zhang et  
 296 al., 2019). For BriqCK, as the opening ratio of the air inlet increased, the SO<sub>2</sub>  
 297 concentration tended to slightly increase. The relatively higher flame temperature  
 298 caused by the larger air inlet opening ratio resulted in a higher conversion rate of fuel  
 299 sulfur to gaseous SO<sub>2</sub>, as has been previously observed (Zhang et al., 2016; Zheng et  
 300 al., 2013).



301

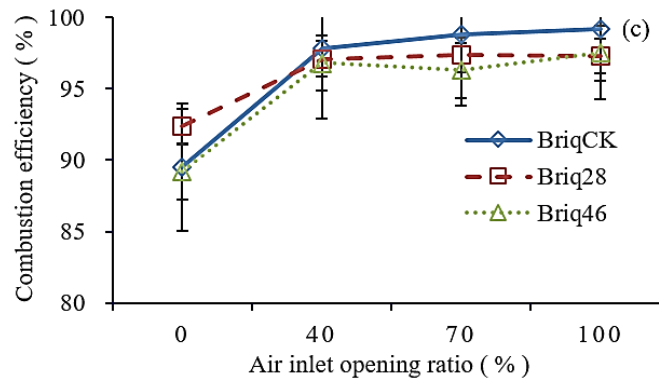
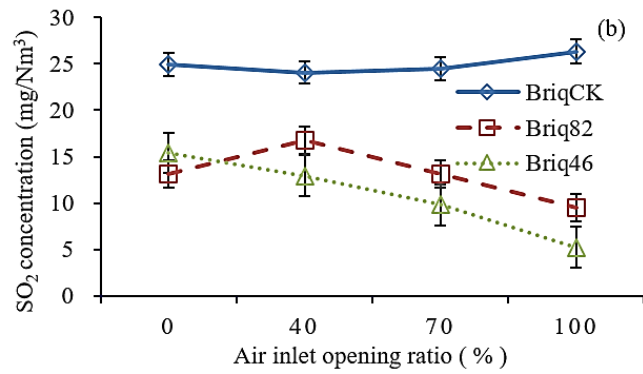


**Fig. 4.** Concentrations of NO<sub>x</sub> (a) and SO<sub>2</sub> (b) and the combustion efficiencies (c) for different honeycomb briquettes.

The concentrations of CO and CO<sub>2</sub> were also used to evaluate the CE according to Equation (3). The CEs of BriqCK, Briq28, and Briq46 are shown in Fig. 4c, respectively. There was a decrease in the CE with the addition of corn stover char. However, the CEs under all experimental conditions, except for the opening ratio of the air inlet of 0 %, exceeded 97.1 %. Although corn stover char addition did not seriously deteriorate the CE in this stove, it may be better to use a specific stove with a secondary airflow for the new fuels, as has been suggested previously (Phusrimuang

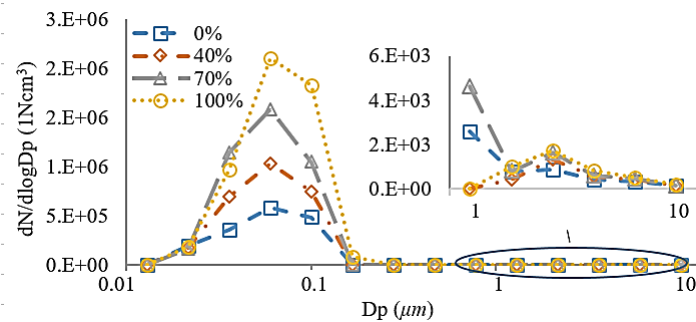
315 et al., 2015; Toscano et al., 2014).

### 316 3.2.2 Total suspended particles emissions

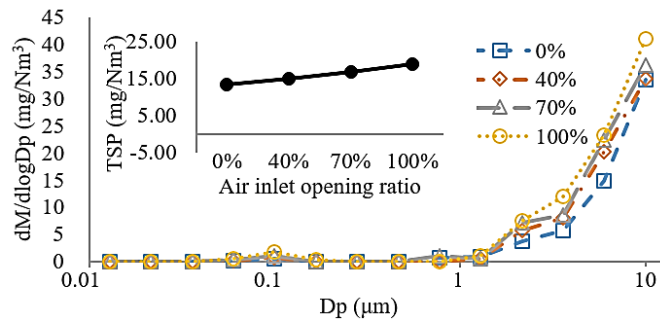
317 Emissions of total suspended particles (TSP), as well as their mass size  
318 concentrations and number size concentrations versus different honeycomb briquettes  
319 and different operating conditions (the air inlet open ratios of 0 %, 40 %, 70 %, and  
320 100 %, respectively), are shown in Fig. 5. The TSP concentrations were 13.45–18.96  
321 mg/Nm<sup>3</sup> for BriqCK, and these increased linearly with the increasing opening ratio of  
322 the air inlet. This might have been related to the rate of burning of the honeycomb  
323 briquettes and airflow speed, as it has been previously revealed that the PM<sub>2.5</sub>  
324 concentration increases under intense flaming conditions for clean-burning stoves  
325 (Wang et al., 2016). The TSP concentrations of Briq28 and Briq46 were 8.82–11.80  
326 mg/Nm<sup>3</sup> and 8.71–11.63 mg/Nm<sup>3</sup>, respectively. As a whole, with the addition of char,  
327 the TSP concentrations decreased; this might have been caused by the lower TSP  
328 emissions of the char compared with those of the semi-coke and the presence of  
329 aluminosilicates in the semi-coke, which were responsible for capturing gaseous  
330 species from the char (Wang et al., 2019).

331 All briquette samples generally presented a similar distribution of mass and  
332 number concentrations at various particle sizes as a function of experimental  
333 conditions, and all the peaks of the number size concentrations occurred at <0.156  
334 μm. PM<sub>10</sub> (<10 μm) mainly consisted of PM<sub>2.5</sub> (<2.5 μm) for all samples, thereby  
335 representing more than 99 % of the total number of particles. A similar distribution

336 was also previously observed by another researcher using wood pellets (Schmidt et  
 337 al., 2018). The peak values of Briq28 and Briq46 were smaller than that for BriqCK.  
 338 Taking the operation conditions with an air inlet opening ratio of 100 % as an  
 339 example, the particle numbers of Briq28 at  $<0.156 \mu\text{m}$  and  $<2.47 \mu\text{m}$  decreased by  
 340 72.4 % and 73.1 %, respectively, compared with those of BriqCK, while those of  
 341 Briq46 decreased by 80.0 % and 80.3 %, respectively. The addition of corn stover  
 342 char reduced the emissions of fine particles ( $\text{PM}_{2.5}$ ), which are known to adversely  
 343 affect human health. The mass size concentration data revealed that most particles  
 344 were larger than  $1.63 \mu\text{m}$ ; when the air inlet opening ratio was 100 %, these particles  
 345 accounted for 95.89 %, 96.51 %, and 96.30 % of the total mass for BriqCK, Briq28,  
 346 and Briq46, respectively. The emission characteristics were distinctly better than  
 347 those of fluid-bed burners owing to the fact that the heating stove was a static  
 348 combustion burner without an air-blast system and the fuels were briquetted (Wang et  
 349 al., 2016).



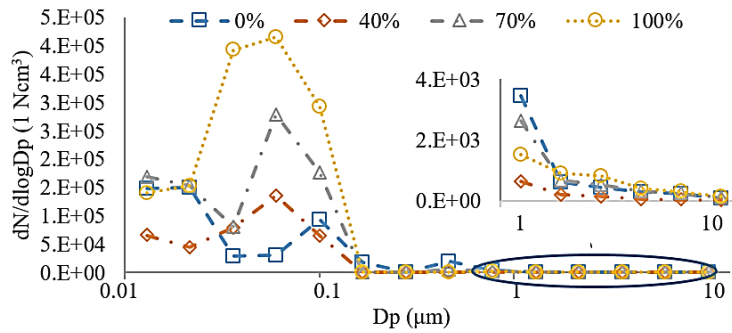
350



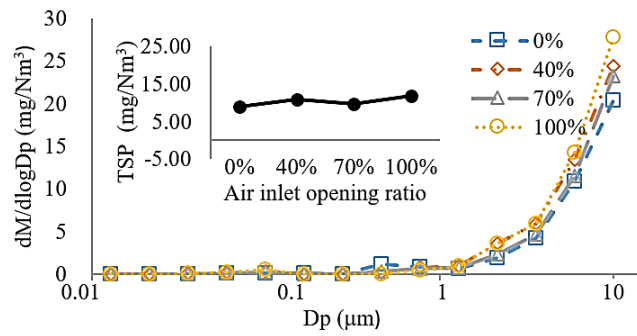
351

352

a. BriqCK



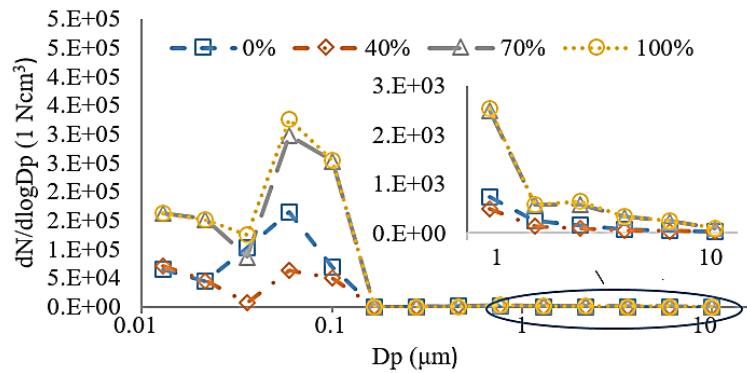
353



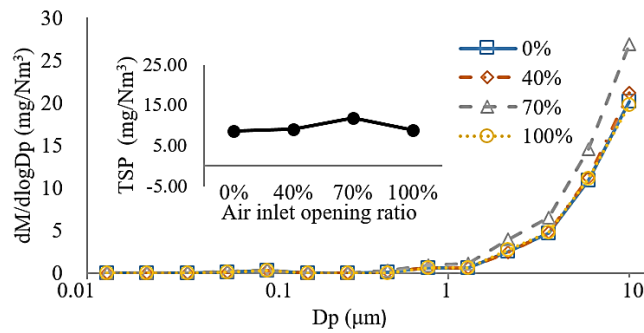
354

355

b. Briq28



356



357

358

c. Briq46

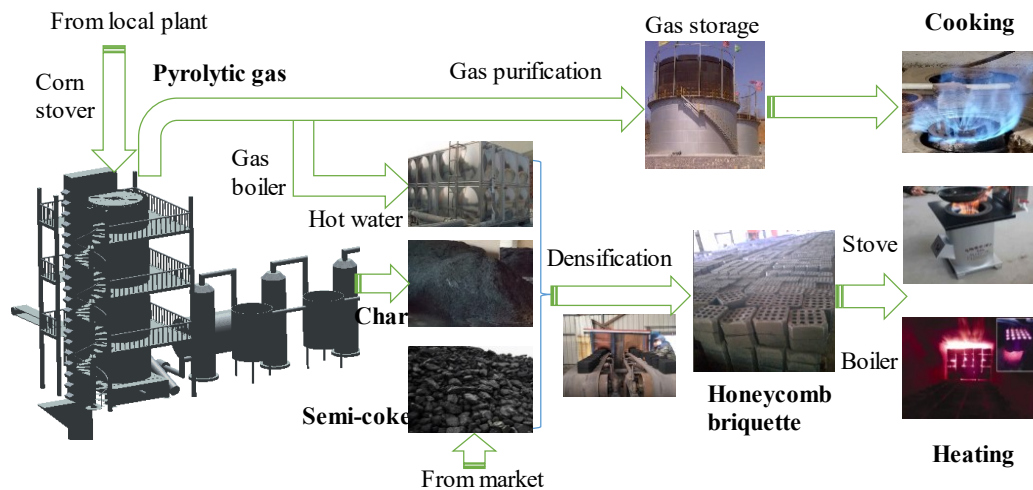
359 **Fig. 5.** Total suspended particles (TSP), number size, and mass size distribution of  
 360 BriqCK (a), Briq28 (b), and Briq46 (c) under different operation conditions (the air  
 361 inlet open ratios of 0 %, 40 %, 70 %, and 100 %, respectively).

### 362 **3.3 Value-chain model design and benefit evaluation**

363 To promote the new heating fuels, which displayed favourable combustion and  
 364 emission performance, a typical value-chain model that was mainly composed of  
 365 straw slow pyrolysis, co-densification of char and semi-coke, and utilization of the  
 366 heating fuels, was designed (Fig. 6). First, crop straws were converted to char,  
 367 pyrolytic gas, and by-products, e.g., tar and a vinegar-like fraction, using pyrolysis  
 368 poly-generation technology. Most of the pyrolytic gas was directly burned in a gas  
 369 burner to produce hot water or hot air for co-densification of the chars and semi-coke,  
 370 and the surplus was purified and delivered to residents as a clean fuel for cooking or  
 371 washing. Most of the chars were blended with semi-coke and molded into honeycomb  
 372 briquettes, which were mainly used for heating via household stoves or boilers. These  
 373 household stoves were widely used in traditional villages, and the boilers were  
 374 suitable for new communities with modern facilities and high population densities in



375 rural China. The remaining fraction of the chars could be used locally as a fertilizer to  
 376 improve soil structure and fertility. The value-chain model was recyclable, highly  
 377 efficient, and clean.



378

379

380 **Fig. 6.** Value-chain model based on honeycomb briquette and straw slow pyrolysis.

381 The benefits evaluation in this study was based on a demonstration project using  
 382 the above value-chain model in Tangshan City, Hebei Province, which went into  
 383 operation in 2017. This plant was mainly comprised of an internal heating straw  
 384 pyrolysis production line, pyrolysis gas purification system, honeycomb briquette  
 385 molding production line, gas burner for hot water or hot air, and two 500 m<sup>3</sup> gas  
 386 storage tanks. A gas pipeline was laid to a nearby village of about 140 households.  
 387 The honeycomb briquette molding production line ran for several years before 2017  
 388 mainly using semi-coke or anthracite as raw materials.

389 In order to add approximately 15–20 % straw char to the honeycomb briquettes of

390 semi-coke, the new investment and running costs for producing straw char are shown  
391 in Table 4. The new investment costs were approximately \$341,000 USD, and the  
392 running costs and income per year were \$220,200 USD and \$67,100 USD,  
393 respectively. The utilization amount of crop-straw was about 4,200 t/y; thus,  
394 approximately 1,260 t of straw char was produced annually. Most pyrolytic gas was  
395 directly burned in a gas burner to produce hot water or hot air, and only about 110,000  
396 m<sup>3</sup> of purified gas was piped to residences for cooking. When the equipment  
397 depreciation period was 10 y, the production cost of straw char was \$134 USD/t, and  
398 the cost would decrease to \$109 USD/t excluding the equipment depreciation costs.  
399 The market prices of semi-coke are about \$121–130 USD/t; therefore, if the new  
400 investment cost of \$341,000 USD or a subsidy of \$25 USD/t of straw char were  
401 supported by national public finance, then the project would be profitable and run  
402 sustainably. The project could increase the income of local farmers by approximately  
403 \$130,200 USD/y through the sale of crop-straws. Complete utilization of the straw  
404 could be achieved, and the rural energy structure and environment would be improved  
405 across the project's region. Thus, the social benefits of the project are considerable.  
406

407 **Table 4.** Estimation of project investment and running costs for straw char production  
408

Items	Details	Income and expenditure	Remarks
New investment (USD)	Straw pyrolysis production line	63,000	The gas pipeline was laid to a nearby village with about 140 households, and the costs of auxiliary equipment (such as
	Gas purification system	12,000	
	Gas boiler for hot water	11,000	

		Gas storage	37,000	stoves) were borne by the residents
		Gas pipeline	210,000	
		Civil engineering	8,000	
		Materials	130,200	
Running	cost	Labor	12,000	
(USD/t)		Electricity	63,000	
		Others	15,000	
		Fuel gas	5,100	Hot water and hot air were used in the
Income (USD/y)		Hot water and hot air	62,000	plant, which allowed cost saving
				compared with the original briquette
				production system
		Production cost of straw char (USD/t)	109	Excluding equipment depreciation costs
			134	Including equipment depreciation costs

409 Note: The equipment depreciation period is 10 y. The sale price of gas is approximately \$0.05 USD/m<sup>3</sup>.

410

#### 411 **4. Conclusions**

412 The co-combustion characteristics of semi-coke and corn stover char combined  
413 in different proportions were tested and analyzed in this study. The results showed  
414 that adding 20 % corn stover char (BS28) effectively improved the combustion  
415 performance of semi-coke, and this proportion was the ideal mixing ratio. Thus, the  
416 integrated combustion characteristics of the blend increased from  $5.44 \times 10^{-12} \text{ K}^{-3} \cdot \text{min}^{-2}$   
417 to  $15.08 \times 10^{-12} \text{ K}^{-3} \cdot \text{min}^{-2}$  for semi-coke.

418 A honeycomb briquette was developed from a combination of semi-coke and  
419 corn stover char for use as a heating fuel in rural China. The emission test results  
420 revealed that SO<sub>2</sub> and PM<sub>2.5</sub> emissions decreased with the addition of corn stover  
421 char; however, NO<sub>x</sub> emissions increased and the CE decreased slightly with corn  
422 stover char addition. The SO<sub>2</sub> concentrations of BriqCK, Briq28, and Briq46 under  
423 different experimental conditions were 24.9–26.3, 9.5–16.7, and 5.2–15.4 mg/Nm<sup>3</sup>,

424 respectively, and the NO<sub>x</sub> concentrations were 63.1–149.7, 54.3–175.4, and 57.7–  
425 168.4 mg/Nm<sup>3</sup>, respectively.

426 A value-chain model for the new heating fuel was developed, and benefits based  
427 on a demonstration project in Tangshan City were analyzed. If the new investment  
428 cost of \$341,000 USD or a subsidy of \$25 US/t of straw char were borne by national  
429 public finance, then the project would be profitable and run sustainably. This study  
430 provided an important technical basis for the development and application of new  
431 heating fuels in China.

432

### 433 **Acknowledgments**

434 The study benefitted from the technical support provided by the Key Laboratory  
435 of Energy Resource Utilization from Agriculture Residue of the Ministry of  
436 Agriculture and Rural Affairs, China. The authors would like to thank the  
437 laboratory' s staff for their support in the successful completion of this work.

438 **Funding:** This work was supported by the China Agriculture Research System [grant  
439 number: CARS-02].

440

### 441 **References**

- 442 Barbanera, M., Cotana, F., Di Matteo, U., 2018. Co-combustion performance and kinetic  
443 study of solid digestate with gasification biochar. *Renew. Energy*. 121, 597–605.
- 444 Chen, X., 2016. Economic potential of biomass supply from crop residues in China. *Appl.*  
445 *Energy*. 166, 141–149. <https://doi.org/10.1016/j.apenergy.2016.01.034>.

446 Cong, H., Yao, Z., Zhao, L., Jia, J., Lan, S., 2017. Development of carbon, gas and oil  
447 polygeneration pilot system based on biomass continuous pyrolysis. *Trans. Chin. Soc. Agric.*  
448 *Eng.* 33, 173–179.

449 Courtemanche, B., Levendis, Y., 1998. A laboratory study on the NO, NO<sub>2</sub>, SO<sub>2</sub>, CO and CO<sub>2</sub>  
450 emissions from the combustion of pulverized coal, municipal waste plastics and tires. *Fuel.*  
451 77, 183–196.

452 De Soete, G.G., 1991. Heterogeneous N<sub>2</sub>O and NO formation from bound nitrogen atoms  
453 during coal char combustion. *Symp. Combust. Proceedings of the 23rd International*  
454 *Symposium on Combustion.* The Combustion Institute. [https://doi.org/10.1016/S0082-](https://doi.org/10.1016/S0082-0784(06)80388-7)  
455 [0784\(06\)80388-7](https://doi.org/10.1016/S0082-0784(06)80388-7)

456 European Biochar Foundation (EBC), 2018. European Biochar Certificate – Guidelines for a  
457 sustainable production of biochar. <http://www.european-biochar.org/en/download> (accessed  
458 30 August 2018).

459 Gómez, N., Rosas, J.G., Cara, J., Martínez, O., Albuquerque, J.A., Sánchez, M.E., 2016.  
460 Slow pyrolysis of relevant biomasses in the Mediterranean Basin. Part 1. Effect of  
461 temperature on process performance on a pilot scale. *J. Clean. Prod.* 120, 181–190.

462 Hu, Q., Shao, J., Yang, H., Yao, D., Wang, X., Chen, H., 2015. Effects of binders on the  
463 properties of bio-char pellets. *Appl. Energy.* 157, 508–516.  
464 <https://doi.org/10.1016/j.apenergy.2015.05.019>.

465 Jie, T., Haiyan, N., Yongming, H., Zhenxing, S., Qiyuan, W., Xin, L., 2018. Primary PM<sub>2.5</sub>  
466 and trace gas emissions from residential coal combustion: Assessing semi-coke briquette for  
467 emission reduction in the Beijing-Tianjin-Hebei region, China. *Atmos. Environ.* 191, 378–  
468 386.

469 Jin, Y., Li, Y., Liu, F., 2016. Combustion effects and emission characteristics of SO<sub>2</sub>, CO,  
470 NO<sub>x</sub> and heavy metals during co-combustion of coal and dewatered sludge. *Front. Environ.*  
471 *Sci. Eng.* 10, 201–210.

472 Klinghoffer, N., Castaldi, M.J., Nzihou, A., 2011. Beneficial Use of ash and char from  
473 biomass gasification. 14 *Proceedings of the 19th Annual North American Waste-to-Energy*  
474 *Conference.* <https://doi.org/10.1115/nawtec19-5421>

475 Kua, H.W., Pedapati, C., Lee, R.V., Kawi, S., 2019. Effect of indoor contamination on carbon  
476 dioxide adsorption of wood-based biochar – Lessons for direct air capture. *J. Clean. Prod.*  
477 210, 860–871.

478 Li, H.J., Zhi, S.W., Li, L.J., Lu, H.E., Yue, M.A., Yuan, L.S., 2016. Comparison of emission  
479 from lantan (semi-coke) instead of raw coal for clean and efficient combustion. *Coal Technol.*  
480 35, 287–289. <https://doi:10.13301/j.cnki.ct.2016.08.118>.

481 Li, L., Zou, D., Xiao, Z., Zeng, X., Zhang, L., Jiang, L., Wang, A., Ge, D., Zhang, G., Liu, F.,  
482 2019. Biochar as a sorbent for emerging contaminants enables improvements in waste  
483 management and sustainable resource use. *J. Clean. Prod.* 210, 1324–1342.  
484 <https://doi.org/10.1016/j.jclepro.2018.11.087>.

485 Li, Q., Li, X., Jiang, J., Duan, L., Ge, S., Zhang, Q., Deng, J., Wang, S., Hao, J., 2016. Semi-  
486 coke briquettes: Towards reducing emissions of primary PM<sub>2.5</sub>, particulate carbon, and carbon  
487 monoxide from household coal combustion in China. *Sci. Rep.* 1, 19306  
488 <https://doi.org/10.1038/srep19306>.

489 Liu, X., Chen, M.Q., Wei, Y.H., 2015. Kinetics based on two-stage scheme for co-  
490 combustion of herbaceous biomass and bituminous coal. *Fuel.* 143, 577–585.

491 Ministry of Agriculture of the People’s Republic of China (MOA), 2016. China’s main crop  
492 straw comprehensive utilization rate exceeds 80 % (in Chinese).  
493 [http://jiuban.moa.gov.cn/zwl/m/zwdt/201605/t20160526\\_5151375.htm](http://jiuban.moa.gov.cn/zwl/m/zwdt/201605/t20160526_5151375.htm) (accessed 26 May  
494 2016).

495 Ministry of Environmental Protection of the People’s Republic of China (MEP), 2016.  
496 Pollution comprehensive management for residential coal combustion (in Chinese).  
497 [http://www.mep.gov.cn/gkml/hbb/bgg/201610/t20161031\\_366528.htm](http://www.mep.gov.cn/gkml/hbb/bgg/201610/t20161031_366528.htm) (accessed 21 May  
498 2016).

499 Moon, C., Sung, Y., Ahn, S., Kim, T., Choi, G., Kim, D., 2013. Effect of blending ratio on  
500 combustion performance in blends of biomass and coals of different ranks. *Exp. Therm. Fluid*  
501 *Sci.* 47, 232–240.

502 Mourant, D., Wang, Z., He, M., Wang, X.S., Garcia-Perez, M., Ling, K., Li, C.Z., 2011.  
503 Mallee wood fast pyrolysis: Effects of alkali and alkaline earth metallic species on the yield  
504 and composition of bio-oil. *Fuel.* 90, 2915–2922.

505 National Energy Administration (NEA), 2016. Notice on printing and distributing the 13th  
506 Five-Year Plan for Energy Development (in Chinese).  
507 [http://www.ndrc.gov.cn/zcfb/zcfbtz/201701/t20170117\\_835278.html](http://www.ndrc.gov.cn/zcfb/zcfbtz/201701/t20170117_835278.html) (accessed 26 December  
508 2016).

509 National Energy Administration (NEA), 2017. Notice on printing and distributing guidance  
510 on promoting biomass energy heating development (in Chinese).  
511 [http://zfxgk.nea.gov.cn/auto87/201712/t20171228\\_3085.htm](http://zfxgk.nea.gov.cn/auto87/201712/t20171228_3085.htm) (accessed 06 December 2017).

512 Niu, S., Chen, M., Li, Y., Song, J., 2017. Co-combustion characteristics of municipal sewage  
513 sludge and bituminous coal. *J. Therm. Anal. Calorim.* 1, 1–14.

514 Peng, X.W., Ma, X.Q., Xu, Z.B., 2015. Thermogravimetric analysis of co-combustion  
515 between microalgae and textile dyeing sludge. *Bioresour. Technol.* 180, 288–295.

516 Phusrimuang, J., Wongwuttanasatian, T., 2016. Improvements on thermal efficiency of a  
517 biomass stove for a steaming process in Thailand. *Appl. Therm. Eng.* 98, 196–202.

518 Ren, X., Sun, R., Meng, X., Vorobiev, N., Schiemann, M., Levendis, Y.A., 2017. Carbon,  
519 sulfur and nitrogen oxide emissions from combustion of pulverized raw and torrefied  
520 biomass. *Fuel.* 188, 310–323. <https://doi.org/10.1016/j.fuel.2016.10.017>.

521 Roy, M.M., Corscadden, K.W., 2012. An experimental study of combustion and emissions of  
522 biomass briquettes in a domestic wood stove. *Appl. Energy.* 99, 206–212.  
523 <https://doi.org/10.1016/j.apenergy.2012.05.003>.

524 Sarkar, P., Sahu, S.G., Mukherjee, A., Kumar, M., Adak, A.K., Chakraborty, N., Biswas, S.,  
525 2014. Co-combustion studies for potential application of sawdust or its low temperature char  
526 as co-fuel with coal. *Appl. Therm. Eng.* 63, 616–623.

527 Schmidt, G., Trouvé, G., Leyssens, G., Schönnenbeck, C., Genevray, P., Cazier, F., Dewaele,  
528 D., Vandenbilcke, C., Faivre, E., Denance, Y., Le Dreff-Lorimier, C., 2018. Wood washing:  
529 Influence on gaseous and particulate emissions during wood combustion in a domestic pellet  
530 stove. *Fuel Process. Technol.* 120, 15–27. <https://doi.org/10.1016/j.fuproc.2018.02.020>.

531 Sun, J., Peng, H., Chen, J., Wang, X., Wei, M., Li, W., Yang, L., Zhang, Q., Wang, W.,  
532 Mellouki, A., 2016. An estimation of CO<sub>2</sub> emission via agricultural crop residue open field  
533 burning in China from 1996 to 2013. *J. Clean. Prod.* 112, 2625–2631.  
534 <https://doi.org/10.1016/j.jclepro.2015.09.112>.

535 Tarelho, L.A.C., Matos, M.A.A., Pereira, F.J.M.A., 2005. The influence of operational  
536 parameters on SO<sub>2</sub> removal by limestone during fluidized bed coal combustion. *Fuel Process.*  
537 *Technol.* 86, 1385–1401.

538 The State Council the People's Republic of China (SCP), 2017. Notice on printing winter  
539 heating plan for the northern region (2017–2021) (in Chinese).  
540 [http://www.gov.cn/xinwen/2017-12/20/content\\_5248855.htm](http://www.gov.cn/xinwen/2017-12/20/content_5248855.htm) (accessed 20 December 2017).

541 Toscano, G., Duca, D., Amato, A., Pizzi, A., 2014. Emission from realistic utilization of  
542 wood pellet stove. *Energy.* 68, 466–650. <https://doi.org/10.1016/j.energy.2014.01.108>.

543 Wang, J., Lou, H.H., Yang, F., Cheng, F., 2016. Development and performance evaluation of  
544 a clean-burning stove. *J. Clean. Prod.* 134(Part B), 447–455.

545 Wang, W., Wena, C., Li, C., Wang, M., Li, X., Zhou, Y., Gong, X., 2019. Emission reduction  
546 of particulate matter from the combustion of biochar via thermal pre-treatment of torrefaction,  
547 slow pyrolysis or hydrothermal carbonization and its co-combustion with pulverized coal.  
548 *Fuel*. 240, 278–288.

549 Werther, J., Saenger, M., Hartge, E.U., Ogada, T., Siagi, Z., 2000. Combustion of agricultural  
550 residues. *Prog. Energy Combust. Sci.* 26, 1–27.

551 Xing, X., Cheng, Z., Li, Y., Zhu, C., Zhang, X., 2019. Co-combustion characteristics and  
552 kinetic analyses of rice straw and pulverized coal. *Chin. J. Process Eng.* 19, 637–643.  
553 <https://doi.org/10.12034/j.issn.1009-606X.218277>.

554 Yank, A., Ngadi, M., Kok, R., 2016. Physical properties of rice husk and bran briquettes  
555 under low pressure densification for rural applications. *Biomass Bioenergy*. 64, 22–30.  
556 <https://doi.org/10.1016/j.biombioe.2015.09.015>.

557 Zhang, S., Jiang, X., Lv, G., 2019. Co-combustion of Shenmu coal and pickling sludge in a  
558 pilot scale drop-tube furnace: Pollutants emissions in flue gas and fly ash. *Fuel Process.*  
559 *Technol.* 184, 57–64.

560 Zhang, S., Jiang, X., Lv, G., Liu, B., Jin, Y., Yan, J., 2016. SO<sub>2</sub>, NO<sub>x</sub>, HF, HCl and PCDD/Fs  
561 emissions during co-combustion of bituminous coal and pickling sludge in a drop tube  
562 furnace. *Fuel*. 186, 91–99.

563 Zhao, P., Shen, Y., Ge, S., Chen, Z., Yoshikawa, K., 2014. Clean solid biofuel production  
564 from high moisture content waste biomass employing hydrothermal treatment. *Appl. Energy*.  
565 131, 345–367.

566 Zheng, D., Lu, H., Sun, X., Liu, X., Han, W., Wang, L., 2013. Reaction mechanism of  
567 reductive decomposition of FGD gypsum with anthracite. *Thermochim. Acta.* 559, 23–31.

568 Declarations of interest: none.  
569